Springer

KSME

Journal of Mechanical Science and Technology 31 (1) (2017) 289~296
www.springerlink.com/content/1738-494x(Print)/1976-3824(Online)
DOI 10.1007/s12206-016-1231-1

A novel stress distribution analytical model of O-ring seals under different properties of materials[†]

Di Wu, Shaoping Wang and Xingjian Wang[*]

School of Automation Science and Electrical Engineering, Beihang University, Beijing, 100191, China

(Manuscript Received January 11, 2016; Revised July 4, 2016; Accepted July 4, 2016)

Abstract

The elastomeric O-ring seals have been widely used as sealing elements in hydraulic systems. The sealing performance of O-ring seals is related to stress distribution. The stresses distribution depends on the squeeze rate and internal pressure, and would vary with properties of O-ring seals materials. Thus, in order to study the sealing performance of O-ring seals, it is necessary to describe the analytic relationship between stress distribution and properties of O-ring seals materials. For this purpose, a novel Stress distribution analytical model (SDAM) is proposed in this paper. The analytical model utilizes two stress complex functions to describe the stress distribution of O-ring seals. The proposed SDAM can express not only the analytical relationship between stress distribution and Young's modulus, but also the one between stress distribution and Poisson's ratio. Finally, compared results between finite element analysis and the SDAM validate that the proposed model can effectively reveal the stress distribution under different properties for O-ring materials.

Keywords: O-ring; Stress distribution; Analytical model; Young's modulus; Poisson's ratio

1. Introduction

The elastomeric O-ring seals have been widely used in hydraulic systems because they are economical and effective. Generally, they are working under squeeze rates and internal pressures. In such case, the stress distribution of O-ring seals has a great impact on the useful life, reliability and controllability. Moreover, the stress distribution is suitable indicator to reflecting the sealing performance [1]. In fact, the stress distribution will be varying with properties of O-ring seals materials. In order to design optimum sealing structure and estimate the useful life, the function relationship between stresses distribution and properties of O-ring seals materials should be analyzed. Especially, when the working condition is specified, the function relationship between stresses field and properties of O-ring seals materials should be concerned. In other words, it is necessary to obtain analytic functions between stresses field and properties under certain boundary condition. Here, the properties of O-ring seals mainly refer to Young's modulus and Poisson's ratio.

The contact stress distribution of seals has been studied extensively by many researchers. Strozzi studied the static stress field in an unpressurized, rounded rectangular, elastomeric seal using both experimental and numerical techniques [2]. Shukla and Nigam presented a numerical- experimental analysis for contact stress problems by photoelastic data [3]. This was only to obtain the contact length and friction factor as the unknown variables for the pure contact stress problem with complete theoretical solutions. Conway concerned the calculations of the distributions of contact pressure between two-dimensional bodies and two transversely isotropic solids [4]. Dragoni proposed a theoretical model which is able to describe the mechanical behavior of an unpressurized, elastomeric O-ring seal inserted into a rectangular groove [5]. Karaszkiewicz gave equations to determine the geometry, the contact pressure and the force of the contact pressure of an O-ring mounted in a seal groove loaded and unloaded by the sealed pressure [6]. Salant and Liao established their models respectively for hydraulic reciprocating seals. The contact stress in their models is obtained by contact mechanics [7]. Those researchers concern stress field of contact surfaces under static sealing. They don't discuss interior stress field of seals. Furthermore, the most of formulas are empirical formula. The mathematical relationship between stress distribution and properties of O-ring seals materials is not discussed detailed.

To find out stress distribution of elastomeric interior seals under uniform squeeze rate, the photoelastic hybrid experimental method is applied to the research. The photoelastic hybrid experimental method was put forward by researcher [8] and used for determining the stress concentration factors and

[*]Corresponding author. Tel.: +86 10 82338917, Fax.: +86 10 82338917
E-mail address: wangxj@buaa.edu.cn
[†]Recommended by Associate Editor Jun-Sik Kim

stress intensity factors by the authors [9]. By this method, Bernard analyzed the internal stresses distribution of X-ring seals under different squeeze rate and internal pressure [10, 11]. Shin analyzed contact length and contact stresses developed in X-rings [12]. Attar investigated failure modes and failure loads in polymeric matrix [13]. For O-ring seals, Namanalyzed the contact stress under 10 % or 20 % squeeze rate using two stress functions [14]. The photoelastic experimental hybrid method determined values of stress functions arguments. Hawongstudied stress field of interior O-ring seals under three kinds of loading conditions [15]. Namdeveloped an O-ring molding method and loading device that will apply a uniform load and internal pressure to the O-ring [16]. Namanalyzed 3-dimensional stress distributions of an O-ring under uniform squeeze rate and internal pressure [17]. Shin designed the proposed transmission-type photoelastic experimental device which can describe actual deformation behavior and the interior stress distributions of O-ring [18]. The stress function in these papers can describe stress distribution precisely. However, the parameters of stress function were determined by photoelastic hybrid experimental data. When the boundary condition is determined without photoelastic hybrid experimental data, the limitation of this method will appear.

In order to solve these issues, in this study, the stress distribution of O-ring seals is analyzed under compressed and laterally one side restrained. A novel Stress distribution analytical model (SDAM) is proposed. This model contains two stress functions which can be utilized to effectively describe the stress distribution of O-ring seals interior. Base on the proposed SDAM, the analytic functions between the stress distribution and properties of O-ring seals materials will be determined under certain boundary condition. The effectiveness of the proposed model is validated by the comparative results with Finite element analysis (FEA).

2. Problem statement and basic theory

The stress problem can be expressed as a half plane problem [19] and affected controllability of system [20, 21]. First of all, the coordinate system is defined. The beginning point of y-axis is set as the middle of contact surface. The direction of y-axis is perpendicular to the contact surface. The x-axis is line through center from upper wall to lower wall. The direction of x-axis is horizontal. The intersection of the y-axis and x-axis is set as the origin. Fig. 1 shows the coordinate system.

The interior stress components in one material had been driven by using the Muskhelishvili complex function [22] and Airy stress functions as follows in:

$$\begin{cases} \sigma_x + \sigma_y = 2\left\{\phi'(z) + \overline{\phi}'(z)\right\} \\ \sigma_y - \sigma_x + 2i\tau_{xy} = 2\left\{\overline{z}\phi''(z) + \psi'(z)\right\} \\ 2\mu\left(u_x + iu_y\right) = \kappa\phi(z) - z\overline{\phi}'(z) - \overline{\psi}(z) \end{cases} \tag{1}$$

where σ_x is stress vector acting along the horizontal direction, σ_y is stress vector acting along the vertical direction, τ_{xy} is shear stress vector, λ is Lamé parameters, μ is shear modulus, u_x is stress vector acting along the horizontal direction, u_y is stress vector acting along the vertical direction.

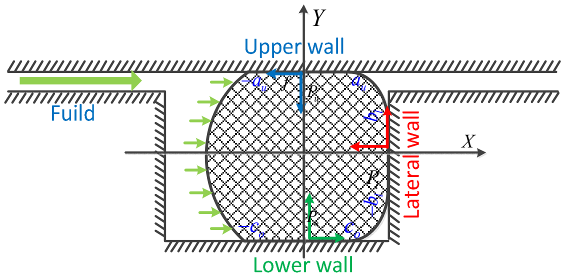

Fig. 1. Global (x, v) and local (x_i, y_i) coordinate systems of O-ring.

Then, Eq. (1) can be expressed as:

$$\begin{cases} \sigma_x = \mathrm{Re}\left[2\phi'(z) - \overline{z}\phi''(z) - \psi'(z)\right] \\ \sigma_y = \mathrm{Re}\left[2\phi'(z) + \overline{z}\phi''(z) + \psi'(z)\right] \\ \tau_{xy} = \mathrm{Im}\left[\overline{z}\phi''(z) + \psi'(z)\right] \end{cases} \tag{2}$$

where Re and Im represent the real and imaginary parts of complex, respectively.

As shown in Eq. (2), stress components are composed of stress functions $\phi(z)$ and $\psi(z)$. If form and parameters of two stress functions are got, the stress distribution functions σ_x and σ_y would be concluded. The analytical functions between stress distribution and properties of O-ring seals materials will be obtained. Therefore, the SDAM is proposed. The form and parameter of the two stress functions $\phi(z)$ and $\psi(z)$ by SDAM.

3. Stress distribution analytical model (SDAM)

Generally, O-ring seals are installed in a groove and compressed by a cover. The contact configuration is regarded as the Hertz contact generally if a plane strain state is assumed. In this case, the contact pressure profile along the horizontal direction of an O-ring seals cross section becomes a semi-ellipse.

In order to calculate stress distribution by two stress function, displacement function will be determined. The deformation of O-ring seals consists of two steps as Fig. 2.

The analytic model of stress distribution is as simple as possible for the purpose of convenient calculation. Moreover, it can reflect relationship between stress distribution and properties of O-ring seals. In order to achieve this aim, the deformation processes of O-ring seals should be analyzed exhaustively and simplified.

The shape change included two steps. The first step is deformation of O-ring seals under preload. The second step is that internal pressure causes deformation of O-ring seals. The

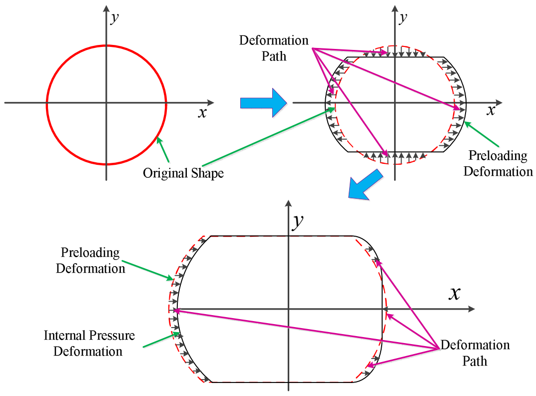

Fig. 2. The change of O-ring seals shape under external force.

deformation of O-ring seals shows as Fig. 2. There are two assumptions during the first step. The first assumption is displacement change of O-ring seals is linear along horizontal and vertical direction. The second assumption is that the displacement is along the x-axis of symmetry. There are two assumptions during the second step. The first assumption is that the displacement change of O-ring seals is linear along horizontal and vertical direction. The second assumption is that the displacement is along the x-axis of symmetry. Based on the above analysis, the parameters of displacement function will be determined. Stress functions $\phi(z)$ and $\chi(z)$ will be got by the method in this paper. Stress distribution of O-ring will calculated out.

According to complex function theory, the displacement function could be describe as :

$$u = \sum_{n=0}^{\infty} c_n z^n \tag{3}$$

where $z = x + yi$, c_n is arbitrary real number constants.

Base on above assumptions, the displacement on the four points could be obtained easily. They are top point, bottom point, right point and origin point. Therefore, four parameters are determined during displacement function.

The displacement functions can be simplified as cubic function:

$$\begin{aligned} u &= c_3 z^3 + c_2 z^2 + c_1 z + c_0 \\ &= c_3\left(x^3 - 3xy^2\right) + c_2\left(x^2 - y^2\right) + c_1 x + c_0 \\ &\quad + \left[c_3\left(3x^2 y - y^3\right) + 2c_2 xy + c_1 y\right] i . \end{aligned} \tag{4}$$

The harmonic function $\phi(z)$ will be expressed as:

$$\phi(z) = d_1 z^3 . \tag{5}$$

Based on Eq. (1), the equation will be concluded:

$$\begin{aligned} 2\mu\left(u_x + iu_y\right) &= \kappa\phi(z) - z\overline{\phi'}(z) - \overline{\psi}(z) \\ &= \kappa d_1 z^3 - 3d_1 z\overline{z}^2 - \overline{\psi}(z) . \end{aligned} \tag{6}$$

Combined with Eqs. (4) and (5) with $d_1 = \frac{2\mu c_3}{\kappa}$, the stress function $\overline{\psi}(z)$ may be written as:

$$\overline{\psi}(z) = 2\mu c_2 z^2 + 2\mu c_1 z - 3d_1 z\overline{z}^2 + c_0 . \tag{7}$$

Eq. (7) can be transformed into:

$$\psi(z) = 2\mu c_2 \overline{z}^2 + 2\mu c_1 \overline{z} - 3d_1 \overline{z} z^2 + c_0 . \tag{8}$$

Both sides of Eq. (8) are differentiated:

$$\psi'(z) = 4\mu c_2 \overline{z} + 2\mu c_1 - 3d_1 \overline{z} z . \tag{9}$$

Now, we have:

$$\begin{aligned} \sigma_x &= 6c_3\left(x^2 - y^2\right) - \left(6c_3 + 3d_1\right)\left(x^2 + y^2\right) \\ &\quad - 4\mu c_2 x - 2\mu c_1 \end{aligned} \tag{10}$$

$$\begin{aligned} \sigma_y &= 6c_3\left(x^2 - y^2\right) + \left(6c_3 - 3d_1\right)\left(x^2 + y^2\right) \\ &\quad + 4\mu c_2 x + 2\mu c_1 \end{aligned} \tag{11}$$

$$\tau_{xy} = -4\mu c_2 y . \tag{12}$$

From the above analysis, stress functions $\phi(z)$ and $\chi(z)$ can be determined as:

$$\begin{cases} \phi(z) = d_1 z^3 \\ \psi(z) = 2\mu c_2 \overline{z}^2 + 2\mu c_1 \overline{z} - 3d_1 \overline{z} z^2 \end{cases} \tag{13}$$

where $d_1 = \frac{2\mu c_3}{\kappa}$.

The parameters of Eq. (13) would be estimated by four points. They are top point, bottom point, right point and left point. Because the O-ring seals are under compressed by preload, the displacement along vertical direction will appear. The displacement along horizontal direction is caused by reason that the O-ring seals is under interior pressure. The some displacement values can be got. The displacement value along vertical direction on the point $(0, y_1)$ is u_{y1}. The displacement value along horizontal direction on the point $(x_1, 0)$ (the rightmost point) is u_{x1}. The displacement value along vertical direction on the point $(x_2, 0)$ (the leftmost point) is u_{x2}.

The parameters matrix will be got:

$$\begin{pmatrix} u_{y1} \\ u_{x1} \\ u_{x2} \end{pmatrix} = \begin{pmatrix} y_1 & 0 & -y_1^3 \\ x_1 & x_1^2 & x_1^3 \\ x_2 & x_2^2 & x_2^3 \end{pmatrix} \begin{pmatrix} c_1 \\ c_2 \\ c_3 \end{pmatrix} . \tag{14}$$

Furthermore, Eq. (14) can be transformed into:

$$\begin{pmatrix} c_1 \\ c_2 \\ c_3 \end{pmatrix} = \begin{pmatrix} y_1 & 0 & -y_1^3 \\ -x_1 & x_1^2 & -x_1^3 \\ x_2 & x_2^2 & x_2^3 \end{pmatrix}^{-1} \begin{pmatrix} u_{y1} \\ u_{x1} \\ u_{x2} \end{pmatrix}. \tag{15}$$

Because the displacement on the upper and lower wall is fixed, the displacement on the point $(0, y_1)$ can be expressed as:

$$u_{y1} = \eta r \tag{16}$$

where η is compressed rate of O-ring seals, r is radius of O-ring seals.

This paper mainly focused on the stress distribution under boundary condition. When the boundary conditions are set and keep consistent, Mullins effect and nonlinear elasticity could be not considered. Therefore, the O-ring seals are as elastomer. The displacement value on the point $(x_1, 0)$ and $(x_2, 0)$ are expressed as:

$$u_{x1} = P/E - 2\eta r \tag{17}$$

$$u_{x2} = -P/E \tag{18}$$

where P is interior pressure, E is Young's modulus.

According to Eqs. (10)-(15), the stress distribution of O-ring will be obtained.

4. Results and discussion

The mechanical properties of O-ring seals and interterm force will be set in order to validate stress distribution model. Elastic modulus of O-ring seals is 15.6 MPa. Poisson's ratio of O-ring seals is 0.49. The radius of O-ring seals is 0.5 mm. The fractional compression of O-ring seals is 20 % with an internal pressure of 1 MPa. Because seal performance mainly depends upon the sealing force, the maximum stress value and stress trend should be paid more attentions and analyzed.

4.1 Stress distribution by FEA

When O-ring seals are deformed under compressed and laterally one side restrained, the stress analysis method is finite element analysis. The FEA is a numerical technique for finding approximate solutions to boundary value problems for partial differential equations. It uses subdivision of a whole problem domain into simpler parts, called finite elements, and variation methods from the calculus of variations to solve the problem by minimizing an associated error function. By this method, Chen [23] established a three-dimensional simplified model for rubber O-sealing ring. The maximum Von Mises stress and contact pressure can be got. Green [24] investigated the stresses distribution of uncompressed O-rings in common cases of restrained and unrestrained geometries. Kim [25] Solved the classical O-ring problem. Aissaoui [26] proposed

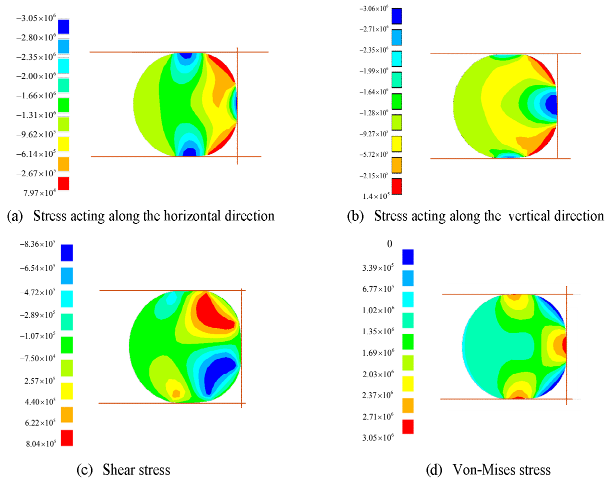

(a) Stress acting along the horizontal direction (b) Stress acting along the vertical direction (c) Shear stress (d) Von-Mises stress

Fig. 3. Stress value obtained from the FEA.

an axisymmetric finite element model which is to simulate the O-ring relaxation behavior. The contact stress profiles and the peak contact stresses are determined versus the time relaxation in order to specify the working conditions thresholds. Therefore, when boundary condition is set, it is good way to analyze stress distribution by FEA. The analysis result by FEA is shown as Fig. 3.

Fig. 3 shows stress distribution under 20 % squeeze rate with an internal pressure of 1 MPa. The stress distribution along the horizontal direction is showed in Fig. 3(a). The maximum of the absolute internal stress will be found in three positions where are middle of upper wall, lower wall and lateral wall. Their maximum values of the absolute internal stress all were about 3.05 MPa. The stress distribution along the vertical direction is showed in Fig. 3(b). It is almost similar to stress distribution along the horizontal direction of Fig. 3(a). The maximum of the absolute internal stress will be found in three positions where are middle of upper wall, lower wall and lateral wall. Their maximum values are greater than that of the absolute internal stress along the horizontal direction by 0.01 MPa. The shear stress distribution is showed in Fig. 3(c). The maximum of the absolute internal stress will be found in middle of upper right part. Its maximum value is about 0.836 MPa. The second maximum of the absolute internal stress will be found in middle of lower right part. Its value is about 0.804 MPa. The von-Mises stress is showed in Fig. 3(d). It is almost similar to stress distribution along the horizontal direction in Fig. 3(b). The maximum of the absolute internal stress will be also found in three positions where are middle of upper wall, lower wall and lateral wall. Their maximum values are about 3.05 MPa. The stress distribution calculated by stress function does not draw stress contours directly. In order to compare between finite element analysis results and SDAM values, the path on the O-ring seals is set firstly, then stress value will map on the path and be plotted as curve. Two straight lines will be set as two paths. The two straight line are represented by the equation $x = 0.3$ and $y = 0.3$.

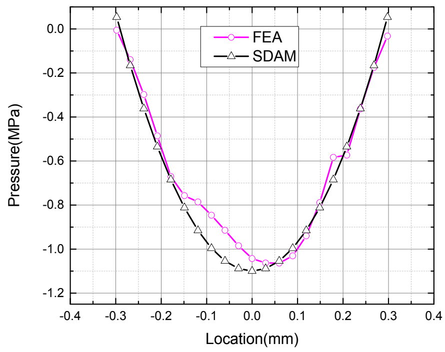

Fig. 4. Stress value along vertical direction.

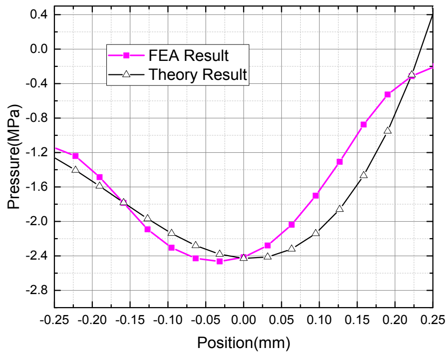

Fig. 5. Stress value along horizontal direction.

4.2 Stress distribution under uniform compressed rate

The stress distribution can be obtained by SDAM based on the boundary condition. Fig. 4 shows stress values along horizontal direction are on the line which is represented by the equation $x = 0.3$. Fig. 5 shows stress values along vertical direction are on the line which is represented by the equation $y = 0.3$.

In the Fig. 4, the circle (—○—) and triangle (—△—) symbols indicate the stress distribution which are obtained from the FEA and theoretical calculation, respectively. The maximum stress absolute value by FEA is about 1.05 MPa and appears on the point (0.05, 0.3). Correspondingly, the maximum stress absolute value by theoretical calculation is about 1.14 MPa and appears on the point (0.3, 0.05). By contrast, the maximums of value by FEA are moved slightly to the right side from the point on the maximums of value by theoretical calculation. Compared FEA results and SDAM values, the maximum stress value and stress trend are almost identical to each other.

In Fig. 5, the circle (—○—) and triangle (—△—) symbols indicate the stress distribution obtained from the FEA and theoretical calculation, respectively. The maximum stress absolute value by FEA is about 2.45 MPa and appears on the point (-0.035, 0.3). Correspondingly, the maximum stress absolute value by theoretical calculation is about 1.14 MPa and appears on the point (0.025, 0.3). By contrast, the curve (—○—) by FEA are moved slightly to the right side from the curve (—△—) which is on the maximums of value by theoretical calculation. Compared between FEA results and SDAM, the maximum stress value and stress trend are similar to each other. The results calculated by SDAM can be express as analytic functions. The stress calculated by two stress functions can reflect stress distribution of O-ring seals. Therefore, the Eqs. (10)-(12) can be described stress distribution as analytic functions.

4.3 Stress distribution under different properties of materials

Eq. (10) can be transform into:

$$\sigma_x = -\left(\frac{3c_3(\lambda+\mu)}{\lambda+3\mu}(x^2+y^2)+4c_2x+2c_1\right)\mu \\ -12c_3y^2 . \tag{19}$$

Eq. (11) can be transform into:

$$\sigma_y = -\left(\frac{3c_3(\lambda+\mu)}{\lambda+3\mu}(x^2+y^2)-4c_2x-2c_1\right)\mu \\ +12c_3x^2 . \tag{20}$$

According to the relationship between Lame constant λ , shear modulus μ , Young's modulus E and Poisson's ratio v :

$$\mu = \frac{E}{2(1+v)} , \quad \lambda = \frac{2Ev}{(1+v)(1-2v)} . \tag{21}$$

Substituting Eq. (21) into Eq. (19), equation will be drawn:

$$\sigma_x = -\left(\frac{3c_3}{3-4v}(x^2+y^2)+4c_2x+2c_1\right) \\ \cdot\frac{E}{2(1+v)}-12c_3y^2 . \tag{22}$$

If point of position and Poisson's ratio are determined, the relationship between stress acting along the horizontal direction and Young's modulus is shown by Eq. (22). The linear relationship between stress along the horizontal direction and Young's modulus will be deduced from Eq. (22). In order to verify the conclusions from Eq. (22), the stress value will be simulated by FEA under the different Young's modulus (from 10 MPa to 15.6 MPa). However, it is difficult that the stress distribution is drawn as stress contours using stress function. For the purpose of comparison of results, the stress data along the horizontal direction on the point (0.04, 0.35) will be saved and plotted as curve under different Young's modulus.

In the Fig. 6 the circle (—○—) and triangle (—△—) symbols indicate the stress values acting along the horizontal direction obtained from the FEA and theoretical calculation,

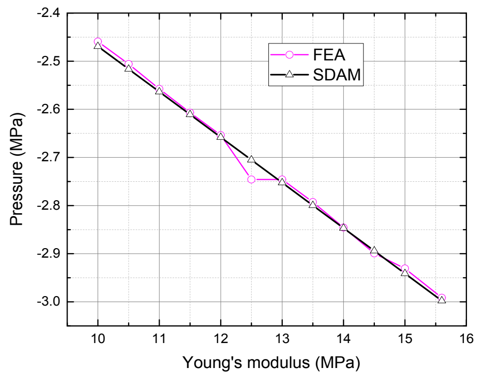

Fig. 6. Stress acting along the horizontal direction with Young's modulus.

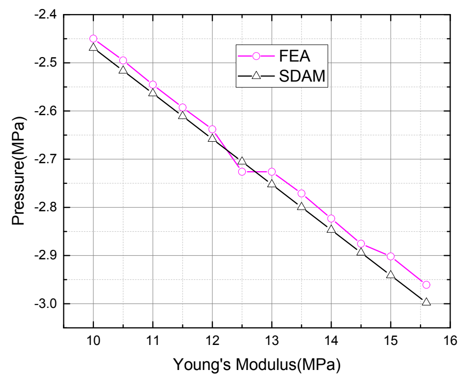

Fig. 7. Stress acting along the vertical direction with Young's modulus.

respectively.

The minimum stress absolute value by FEA is about 2.45 MPa when Young modulus of O-ring seals is 10 MPa. The maximum stress absolute value by FEA is about 3 MPa when Young modulus of O-ring seals is 15.6 MPa. By comparison, the minimum stress absolute value by theory analysis is about 2.44 MPa when Young modulus of O-ring seals is 10 MPa. The maximum stress absolute value by theory analysis is about 3 MPa when Young modulus of O-ring seals is 15.6 MPa.

As shown in the Fig. 6, a linear relationship appears between stress values on the point and Young's modulus. It is found that the function relationship between the results from the FEA and that from the theory are nearly the same.

Substituting Eq. (21) into Eq. (20), leads to:

$$\sigma_y = -\left(\frac{3c_3}{3-4v}\left(x^2+y^2\right)-4c_2x-2c_1\right)\cdot\frac{E}{2(1+v)}+12c_3x^2 . \tag{23}$$

Also similar to the previous analysis, if point of position and Poisson's ratio are determined, the relationship between stress acting along the vertical direction and Young's modulus is shown by Eq. (23). The relationship between stress along the vertical direction and Young's modulus is also linear from the Eq. (23). In order to verify the conclusions from Eq. (23), the stress value along the vertical direction will be simulated by FEA under the different Young's modulus (from 10 MPa to 15.6 MPa). For the purpose of comparison of results, the stress value along the vertical direction on the point (0.04, 0.35) will be saved and plotted as curve.

In the Fig. 7 the circle (—○—) and triangle (—△—) symbols indicate the stress values acting along the vertical direction obtained from the FEA and theoretical calculation, respectively.

The minimum stress absolute value by FEA is about 2.45 MPa when Young modulus of O-ring seals is 10 MPa. The maximum stress absolute value by FEA is about 2.95 MPa when Young modulus of O-ring seals is 15.6 MPa.

By comparison, the minimum stress absolute value by theory analysis is about 2.46 MPa when Young modulus of O-ring seals is 10 MPa. The maximum stress absolute value by theory analysis is about 3 MPa when Young modulus of O-ring seals is 15.6 MPa.

As can be seen from the Fig. 7, a linear relationship appears between stress values on the point and Young's modulus. The data by FEA is almost identical to the data by theoretical analysis.

In order to study the relationship between stress along the horizontal direction and Poisson's ratio, the Eq. (19) can be transformed into:

$$\sigma_x = -\frac{6c_3E}{7(3-4v)}\left(x^2+y^2\right)-\frac{E}{14(1+v)}\left(c_3x^2+c_3y^2+4c_2x+2c_1\right)-12c_3y^2 . \tag{24}$$

If point of position and Young's modulus are determined, the relationship between stress acting along the horizontal direction and Poisson's ratio is shown by Eq. (24). In order to verify the conclusions from Eq. (24), the stress value will be simulated by FEA under the different Poisson's ratio (from 0.27 to 0.49). For the purpose of comparison of FEA result and SDAM values, the stress values along the horizontal direction on the point (0.04, 0.35) are saved and plotted as curve.

In the Fig. 8 the circle (—○—) and triangle (—△—) symbols indicate the stress values acting along the horizontal direction obtained from the FEA and theoretical calculation under different Poisson's ratio, respectively.

The minimum stress absolute value by FEA is about 2.95 MPa when Poisson's ratio of O-ring seals is 0.31. The maximum stress absolute value by FEA is about 3 MPa when Poisson's ratio of O-ring seals is 0.48. By comparison, the minimum stress absolute value by theory analysis is about 2.46 MPa when Poisson's ratio of O-ring seals is 0.27. The maximum stress absolute value by theory analysis is about 3.01 MPa when Poisson's ratio of O-ring seals is 0.49.

The relationship between stress values on the point and re-

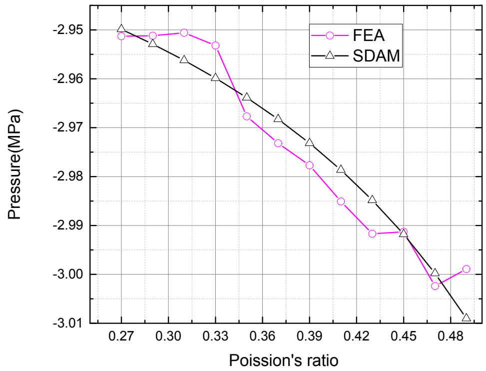

Fig. 8. Stress acting along the horizontal direction with Poission's ratio.

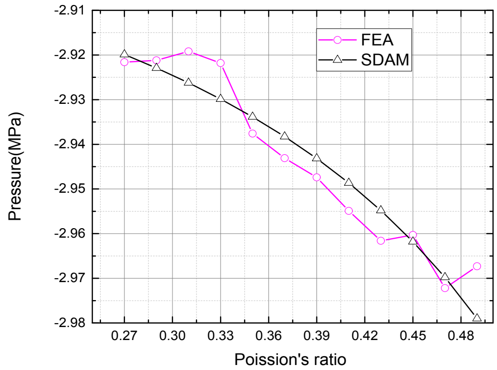

Fig. 9. Stress acting along the vertical direction with Poission's ratio.

ciprocal for Poisson's ratio appear linear. As can be seen from the Fig. 8, although the data by FEA is not identical to the data by theoretical analysis, the maximum error is about 0.01 Mpa when Poisson's ratio of O-ring seals is 0.49. The stress distribution which is calculated by two stress function in this paper can be considered as good approximation.

For the relationship between stress along the vertical direction and Poisson's ratio, the Eq. (20) can be transformed into:

$$\sigma_y = -\frac{6c_3E}{7(3-4v)}\left(x^2+y^2\right) - \frac{E}{14(1+v)}\left(c_3x^2+c_3y^2-4c_2x-2c_1\right)+12c_3x^2 . \tag{25}$$

If point of position and Young's modulus are determined, the relationship between stress acting along the vertical direction and Poisson's ratio is shown by Eq. (24). From Eq. (24) the relationship between stress values on the point and reciprocal for Poisson's ratio appear linear. In order to verify the conclusions, the stress value will be simulated by FEA under the different Poisson's ratio (from 0.27 to 0.49). The stress values along the horizontal direction on the point (0.04, 0.35) are saved and plotted as curve.

In the Fig. 9, the circle (—○—) and triangle (—△—) symbols indicate the stress values acting along the vertical direction obtained from the FEA and theoretical calculation under different Poisson's ratio, respectively.

The minimum stress absolute value by FEA is about 2.92 MPa when Poisson's ratio of O-ring seals is 0.31. The maximum stress absolute value by FEA is about 2.97 MPa when Poisson's ratio of O-ring seals is 0.48. By comparison, the minimum stress absolute value by theory analysis is about 2.92 MPa when Poisson's ratio of O-ring seals is 0.27. The maximum stress absolute value by theory analysis is about 2.98 MPa when Poisson's ratio of O-ring seals is 0.49.

As shown in the Fig. 9, the data by FEA is not identical to the data by theoretical analysis. However, the maximum error is about 0.01 Mpa when Poisson's ratio of O-ring seals is 0.49. The stress distribution which is calculated by two stress function in this paper can be considered as good approximation.

5. Conclusion

The novel SDAM has been proposed to describe the analytical function between stress distribution and properties of an elastomeric O-ring seals under certain boundary condition. In the proposed model, first of all, the deformation behavior of O-ring seals was analyzed under compressed and laterally one side restrained. According to deformation analysis and SDAM, the form and parameters of analytical function between stress distribution and properties will be determined. When the boundary condition is set, the analytical function will be readily determined by SDAM. The comparison with finite element analysis shows that SDAM can reflect maximum stress value and stress trend with properties for O-ring seals materials. The effectiveness of the proposed model can be validated.

Acknowledgment

This work is supported by the National Basic Research Program of China (973 Program) (Grant No. 2014CB046402), the National Natural Science Foundation of China (Grant Nos. 51620105010, 51675019, 51575019) and the Program 111 of China.

References

[1] F. Theyse, The inverse hydrodynamic theory and its application in the design of controlled leakage seals between moving parts, *Proc. 3rd Int. Conf. on Fluid Sealing F* (1967) 17-32.

[2] A. Strozzi, Static stresses in an unpressurized, rounded, rectangular, elastomeric seal, *Asle Transactions*, 29 (4) (1986) 558-564.

[3] A. Shukla and H. Nigam, A numerical-experimental analysis of the contact stress problem, *The Journal of Strain Analysis for Engineering Design*, 20 (4) (1985) 241-245.

[4] H. D. Conway, The pressure distribution between two elastic bodies in contact, *Zeitschrift für Angewandte Mathematik und Physik (ZAMP)*, 7 (5) (1956) 460-465.

[5] E. Dragoni and A. Strozzi, Theoretical analysis of an unpressurized elastomeric O-ring seal inserted into a rectangular groove, *Wear*, 130 (1) (1989) 41-51.

[6] A. Karaszkiewicz, Geometry and contact pressure of an O-ring mounted in a seal groove, *Industrial & Engineering Chemistry Research*, 29 (10) (1990) 2134-2137.
[7] C. Liao, W. Huang, Y. Wang, S. Suo and Y. Liu, Fluid-solid interaction model for hydraulic reciprocating O-ring seals, *Chinese Journal of Mechanical Engineering*, 26 (1) (2013) 85-94.
[8] H. Kopecki and J. Smykla, Experimental-numerical hybrid technique for stress analysis of plates with holes in post buckling state, *Experimental Stress Analysis*, Springer (1986) 271-280.
[9] J. S. Hawong, D. C. Shin and H. J. Lee, Photoelastic experimental hybrid method for fracture mechanics of anisotropic materials, *Experimental Mechanics*, 41 (1) (2001) 92-99.
[10] A. O. Bernard, J. S. Hawong, D. C. Shin and H. S. Lim, Internal stress distribution of X-ring using photoelastic experimental hybrid method, *Journal of Mechanical Science and Technology*, 28 (5) (2014) 1697-1708.
[11] A. O. Bernard, J. S. Hawong, D. C. Shin and B. Dong, Contact behavior analysis of elastomeric x-ring under uniform squeeze rate and internal pressure before and after forcing-out using the photoelastic experimental hybrid method, *Journal of Mechanical Science and Technology*, 29 (5) (2015) 2157-2168.
[12] D. C. Shin, J. S. Hawong, S. W. Lee, A. O. Bernard and H.-S. Lim, Contact behavior analysis of X-ring under internal pressure and uniform squeeze rate using photoelastic experimental hybrid method, *Journal of Mechanical Science and Technology*, 28 (10) (2014) 4063-4073.
[13] M. M. Attar, F. Barati, M. Ahmadpour and E. Rezapour, Failure analysis of unidirectional polymeric matrix composites with two serial pin loaded-holes, *Journal of Mechanical Science and Technology*, 30 (6) (2016) 2583-2591.
[14] J. Nam, J. Hawong, S. Han and S. Park, Contact stress of O-ring under uniform squeeze rate by photoelastic experimental hybrid method, *Journal of Mechanical Science and Technology*, 22 (12) (2008) 2337-2349.
[15] J. Hawong, J. Nam, S. Han, O. Kwon and S. Park, A study on the analysis of O-ring under uniform squeeze rate and internal pressure by photoelastic experimental hybrid method, *Journal of Mechanical Science and Technology*, 23 (8) (2009) 2330-2340.
[16] J. H. Nam, J. S. Hawong, K. H. Kim, O. S. Kwon and S.-H. Park, A study on the development of a loading device using a photoelastic stress freezing method for the analysis of O-ring stress, *Journal of Mechanical Science and Technology*, 24 (3) (2010) 693-701.
[17] J. Nam, J. Hawong, Y. Liu and D. Shin, 3-Dimensional stress analysis of O-ring under uniform squeeze rate and internal pressure by photoelastic experimental hybrid method, *Journal of Mechanical Science and Technology*, 25 (9) (2011) 2447-2455.
[18] D. C. Shin, J. H. Nam and D. W. Kim, Experimental interior stress fields of a constantly squeezed O-ring modeling from hybrid transmission photoelasticity, *Experimental Techniques* (2013).
[19] A. Sackfield, D. Hills and D. Nowell, *Mechanics of elastic contacts*, Elsevier (2013).
[20] X. Wang and S. Wang, Adaptive fuzzy control with smooth inverse for nonlinear systems preceded by non-symmetric dead-zone, *International Journal of Systems Science*, 47 (9) (2016) 2237-2246.
[21] X. Wang and S. Wang, Output torque tracking control of direct-drive rotary torque motor with dynamic friction compensation, *Journal of the Franklin Institute*, 352 (11) (2015) 5361-5379.
[22] N. I. Muskhelishvili, *Some basic problems of the mathematical theory of elasticity*, Springer Science & Business Media (2013).
[23] J. Z. Chen, M. X. Huang and X. R. Wang, Non-linear finite element analysis on rubber O-sealing ring of SRM, *Advanced Materials Research* (2015) 490-494.
[24] I. Green and C. English, Stresses and deformation of compressed elastomeric O-ring seals, *14th International Conference on Fluid Sealing*, Firenze, Italy (1994) 6-8.
[25] H. K. Kim, S. H. Park, H. G. Lee, D. R. Kim and Y. H. Lee, Approximation of contact stress for a compressed and laterally one side restrained O-ring, *Engineering Failure Analysis*, 14 (8) (2007) 1680-1692.
[26] H. Aissaoui, M. Diany and J. Azouz, Numerical simulation of radial and axial compressed elastomeric O-ring relaxation, *Global Journal of Researches In Engineering*, 12 (4-A) (2012).

Di Wu is currently a Ph.D. candidate in Mechatronics Engineering of Beihang University, China. His main research interests are dynamic fracture mechanics, stress analysis, thermal analysis etc.

Shaoping Wang received the Ph.D., M.Eng. and B.Eng. degrees in Mechatronics Engineering from Beihang University, China, in 1994, 1991 and 1988. She has been with the Automation Science and Electrical Engineering at Beihang University since 1994 and promoted to the rank of Professor in 2000. Her research interests include engineering reliability, fault diagnostic, prognostic and health management, active fault tolerant control.

Xingjian Wang received the Ph.D. and B.Eng. degrees in mechatronics engineering from Beihang University, China, in 2012 and 2006. He is currently with the School of Automation Science and Electrical Engineering, Beihang University, Beijing, China. His research interests include nonlinear control, fault diagnostic, prognostic and health management, fault tolerant control.